DOI: 10.19884/j.1672-5220.202604012

Effect of Cotton Waste-Based MCC on Interface and Mechanical Properties of Jute/Glass Fiber-Reinforced Epoxy Composites

LI Hongyang, YANG Jiahua, WANG Zechuan, YAO Lan, WANG Ni*
College of Textiles, Donghua University, Shanghai 201620, China

Abstract: With the increasingly prominent issues of energy shortage and environmental pollution, it has become imperative to develop natural fiber-reinforced composites for applications in infrastructure, automobiles, etc. In this study, jute fibers, as low-cost natural fibers, were selected as the reinforcement for the composites. To enhance the overall mechanical properties, glass fibers were also added as the reinforcement to form the hybrid composites. To improve the interfacial properties between the fibers and the epoxy resin, the microcrystalline cellulose (MCC) prepared from cotton waste was employed to modify the composites. The introduction of MCC in the designed four jute/glass epoxy composites changed the mechanical properties. Especially for the composite with two layers of glass fiber fabrics on each of the top and bottom surfaces and two layers of jute fabrics in the middle (designated as 2G2J2G), its bending strength and bending modulus after MCC addition reached 113.66 MPa and 11.87 GPa, respectively, which were 34.19% and 23.26% higher than those of the composite without MCC. Scanning electron microscopy (SEM) observations revealed that MCC was uniformly dispersed in the epoxy resin matrix, which would have a positive effect on the interfacial strengthening.

Keywords: natural fiber-reinforced composite; microcrystalline cellulose; jute; glass fiber; interface performance
CLC number: TB332 **Document code**: A
Article ID: 1672-5220(2026)05-0071-09

0 Introduction

Driven by the green and sustainable development strategy, the research and development of natural fiber-reinforced composites has become an important research direction in materials science[1-5]. Among various natural fibers, bast fibers are often used as reinforcements in natural fiber-reinforced composites due to their wide availability and low cost[6-9]. However, compared with synthetic fibers, bast fibers exhibit lower mechanical properties and poor interfacial bonding with the resin matrix, which limits their further development and utilization. To address the drawback of low mechanical properties of bast fibers, the design of hybrid composites offers a favorable synergistic strategy[10-12]. By introducing high-strength and high-modulus synthetic fibers to hybridize with natural fibers, the complementary advantages of the different fiber components can significantly enhance the overall load-bearing capacity of the composites.

The interfacial issues in fiber-reinforced composites have also received widespread attention[13-16]. Effective interfacial modification can positively contribute to the enhancement of the mechanical properties of the final composite. Numerous studies have shown that introducing cellulose onto the fiber surface or into the matrix material is considered a feasible strategy to improve the interfacial performance between fibers and the matrix[17-18]. Jabbar et al.[19] coated jute fabrics with prepared nanocellulose suspensions of different concentrations to fabricate nanocellulose-coated jute/green epoxy composites. The results showed that the composites with nanocellulose coating exhibited increased tensile modulus, bending strength, bending modulus, and fracture toughness. Asadi et al.[20] coated glass fibers with cellulose nanocrystals to prepare glass fiber/epoxy composites and evaluated their interfacial and mechanical properties. The results indicated that the glass fiber-reinforced composites with cellulose nanocrystal coating improved interfacial properties, with a 69% increase in interfacial shear strength, a 10% increase in tensile strength, and 43% and 40% increases in bending strength and bending modulus, respectively. Bandaru et al.[21] proposed a method to improve the mechanical and dynamic mechanical properties of flax-reinforced novel methyl methacrylate and polyurethane composites using microcrystalline cellulose (MCC). Different mass fractions of MCC were dispersed into the matrix, and the composites were fabricated via the vacuum infusion method. The study demonstrated that the addition of MCC into the matrix significantly improved the fiber/matrix interface, enhancing the in-plane shear strength, interlaminar shear strength, and bending strength of the

Received date: 2026-04-20
* Correspondence should be addressed to WANG Ni, email: wangni@dhu.edu.cn
Citation: Li H Y, Yang J H, Wang Z C, et al. Effect of cotton waste-based MCC on interface and mechanical properties of jute/glass fiber-reinforced epoxy composites [J]. *Journal of Donghua University (English Edition)*, 2026, 43(5): 71-79.

composites.

In this study, jute fibers were selected as the reinforcement. To compensate for the insufficient mechanical properties of jute fibers, a small amount of glass fibers was introduced to form a hybrid system. Four types of jute/glass hybrid fiber-reinforced epoxy composites were designed. Meanwhile, to improve the interfacial adhesion between fibers and resin, MCC derived from cotton waste was added, and its structure and properties were characterized. In addition, the tensile and bending properties of the composites before and after MCC modification were tested, and the fracture morphologies of the composites were observed.

1 Materials and Methods

1.1 Materials

The cotton waste was recycled from the carding machine. It had an upper half mean length of 17.4 mm, a short fiber mass fraction of 99%, a breaking tenacity of 20.7 cN/tex, and a trash content of 5 particles per gram. The basic structural parameters of the jute fabric and glass fiber fabric are shown in Table 1. The epoxy adhesive film was purchased from Shanghai Huayi Resin Co., Ltd., China. Sodium hydroxide (NaOH, AR, purity no less than 96%) and sulfuric acid (H_2SO_4, AR, purity no less than 98%) were purchased from Sinopharm Chemical Reagent Co., Ltd., China.

Table 1 Basic structural parameters of fabric samples

Sample	Warp count/(end/10 cm)	Weft count/(pick/10 cm)	Thickness/mm	Areal density/(g/m^2)
Jute fabric	59.2±0.4	76.4±0.5	1.26±0.01	407.42±11.03
Glass fiber fabric	136.5±0.7	160.0±1.2	0.20±0.01	203.78±1.47

1.2 Preparation of MCC

The cotton waste was cut into pieces smaller than 1 cm. The cleaned cotton waste was added to a 5% (mass fraction) NaOH solution at a liquid-to-solid ratio of 40 mL/g and magnetically stirred in a constant temperature (70 ℃) oil bath for 4 h. The mixture was then neutralized and suction filtered. An appropriate amount of the filter residue was dried and added to a 55% (mass fraction) H_2SO_4 solution at a liquid-to-solid ratio of 30 mL/g. Then the solution was heated to 50 ℃, and stirred for 2 h. The resulting solution was diluted tenfold and centrifuged at 11 000 r/min for 10 min. The supernatant was discarded, and the precipitate was washed with deionized water. This centrifugation and washing process was repeated at least five times until the solution became neutral. The product was dried and ground into a powder to obtain MCC.

1.3 Characterization of MCC

A scanning electron microscope (FlexSEM 1000, Hitachi High-Technologies Corporation, Japan) was used to observe the surface morphology of cotton waste, MCC, and commercial microcrystalline cellulose (CMCC). A laser particle size analyzer (PSA1190 L, Anton Paar, Austria) was used to measure the particle size and distribution of MCC and CMCC. A Fourier transform infrared (FTIR) spectrometer (Spectrum Two, PerkinElmer, UK) was used to analyze the chemical composition of cotton waste, MCC, and CMCC. A thermogravimetric analyzer (TGA4000, PerkinElmer, USA) was used to test the thermal stability of cotton waste, MCC, and CMCC. An X-ray diffractometer (D8 Advance, Bruker AXS, Germany) was used to analyze the crystal structures of MCC and CMCC, and the crystallinity of the samples was calculated as

$$C_{rl} = \frac{I_{002} - I_{am}}{I_{002}} \times 100\%, \quad (1)$$

where C_{rl} indicates the relative crystallinity; I_{002} is the diffraction peak intensity of the (002) crystal plane, corresponding to $2\theta = 22.6°$, indicating the diffraction intensity of the crystalline region; I_{am} is the diffraction peak intensity at $2\theta = 18.0°$, which is the diffraction intensity of the amorphous region.

1.4 Composite design

Based on the fabric areal density, the hybrid mass ratio of jute fabric to glass fiber fabric was determined as 1 ∶ 2. An eight-layer glass fiber-reinforced epoxy composite (8G) and a four-layer jute fiber-reinforced epoxy composite (4J) were set as references. Two types of six-layer jute/glass hybrid composites were designed. The detailed layup configurations are shown in Fig. 1, where jute fabrics and glass fiber fabrics are designated as J and G, respectively, and the number preceding the letter represents the number of layers of the corresponding fabrics. 2G1J2G1J denotes the composite with a sequential arrangement of two layers of glass fiber fabrics, one layer of jute fabric, two layers of glass fiber fabrics, and one layer of jute fabric. 2G2J2G denotes the composite with a sequential arrangement of two layers of glass fiber fabrics, two layers of jute fabrics, and two layers of glass fiber fabrics.

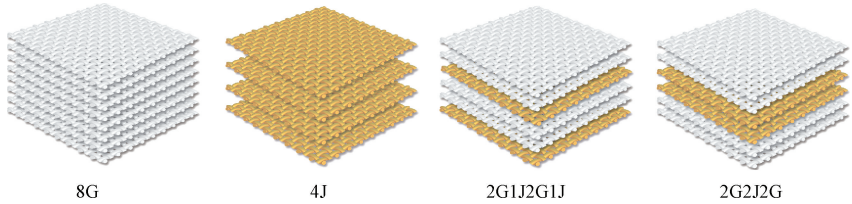


Fig. 1 Schematic illustration of composite layup configurations

1.5 Composites manufacturing

MCC modified jute/glass fiber-reinforced epoxy composites were prepared by compression molding using a compression molding machine (XLB-400 × 400 × 2, Shanghai Qicai Hydraulic Machinery Co., Ltd., China). Before preparation, the MCC powder was dried in a vacuum oven at 80 ℃ for 2 h to remove moisture, and then sieved through a 200-mesh screen to avoid agglomeration. Based on previous experimental results, MCC was added to the surfaces of jute and glass fiber fabrics at mass fractions of 2%, 4%, and 6%. The composites achieved the highest tensile strength at an MCC mass fraction of 4%; therefore, this mass fraction was selected. Hereafter, all percentages of MCC refer to mass fractions. As shown in Fig. 2, 4% MCC powder was evenly sprayed onto the fabric surface. Before compression molding, the stacked plies were placed into a custom mold and sandwiched between polyimide (PI) films. The heating temperature was 130 ℃, the pressure was 2.5 MPa, and the pressing time was 2 h.

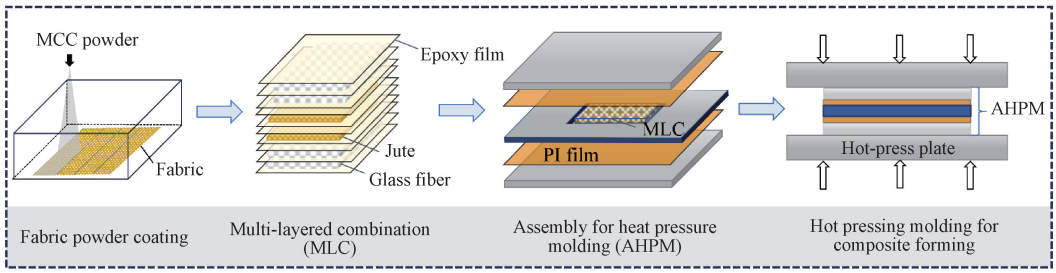


Fig. 2 Schematic illustration of hot-pressing molding process for composite manufacturing

1.6 Mechanical property test

Tensile and bending properties were tested in accordance with ASTM D3039 and ASTM D7264, respectively. Before testing, the composites were conditioned for 24 h in a constant temperature and humidity chamber ((25 ± 2) ℃, (65 ± 2)% relative humidity). Testing was conducted using an electronic universal testing machine (Model 4302, Instron, USA), with five valid specimens per group.

1.7 Morphology characterization

The fracture cross-sections of the composites were examined at various magnifications using an optical microscope (NIKON SMZ745, Japan) and a scanning electron microscope (TM-3000, Hitachi, Japan). Micrographs were captured of appropriate regions for comparative analysis. Before scanning electron microscopy (SEM) observation, the specimens were coated with gold sputtering to enhance their surface conductivity.

2 Results and Discussion

2.1 Physicochemical characterization results of MCC

Figure 3 shows the surface morphologies of cotton waste before and after alkali treatment, MCC, and CMCC. It can be seen from Fig. 3 that after alkali treatment, the cotton fibers exhibit fewer surface impurities and a smoother surface. The MCC prepared by hydrolysis presents two distinct morphologies: ribbon-shaped and rod-shaped. In addition, both MCC and CMCC contain a small number of fragments and small particles. This was because during hydrolysis, the network structure of cellulose was gradually destroyed, with the amorphous regions being decomposed, and the fibers were broken into small fragments, forming irregular particles.

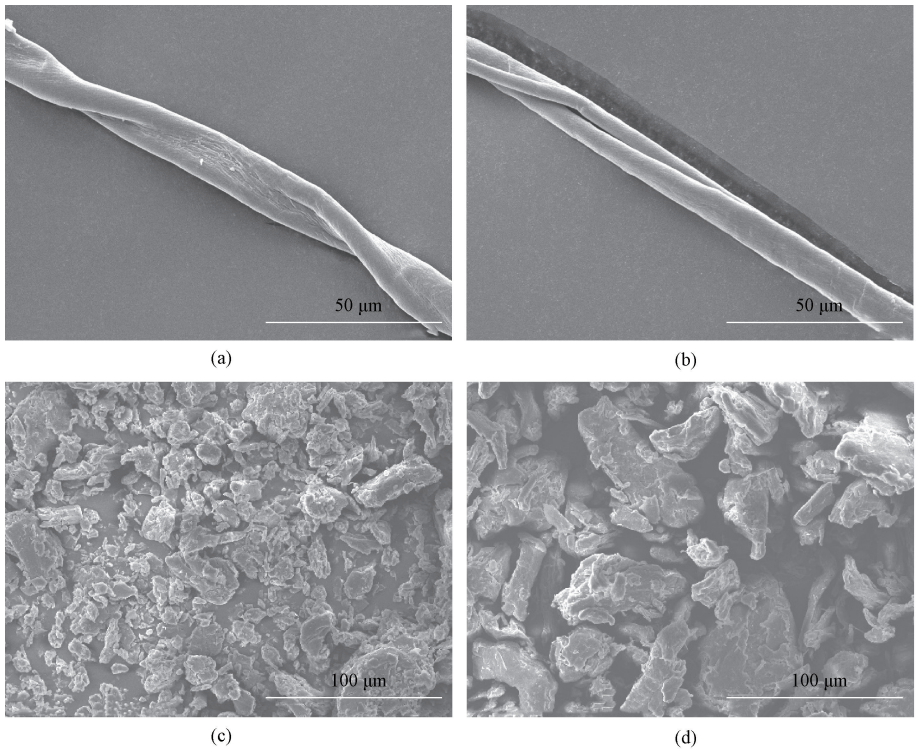


Fig. 3 SEM images: (a) cotton waste before alkali treatment; (b) cotton waste after alkali treatment; (c) MCC; (d) CMCC

Figure 4 presents the characterization results of the samples, including particle sizes, X-ray diffraction (XRD) patterns, Fourier transform infrared (FTIR) spectra, and thermogravimetric (TG) results. The degree of hydrolysis of cotton waste to MCC was assessed by particle size and distribution. As shown in Fig. 4(a), the particle sizes of both CMCC and the prepared MCC are mainly distributed between 1 and 100 μm, with average sizes of 34.71 μm and 26.53 μm, respectively. The size difference was primarily attributed to the raw material type and processing conditions. Figure 4(b) shows that MCC exhibits a similar XRD pattern to CMCC, except for two peaks at 2θ near 15°, corresponding to the same crystal planes at 14.6° and 16.3°. Both MCC and CMCC display characteristic peaks at 22.6° and 34.5°, assigned to the (002) and (040) crystal planes, respectively, which are typical characteristics of cellulose I. Calculations show that the crystallinity values of MCC and CMCC are 89.53% and 78.27%, respectively. MCC exhibited high crystallinity because the hydronium ions from the acid preferentially attacked and cleaved the β-1, 4-glycosidic bonds within the structurally disordered amorphous regions. This selective hydrolysis removed the amorphous domains while leaving the highly ordered crystalline regions intact, thereby yielding MCC with high crystallinity. Higher crystallinity led to superior strength, stiffness, dimensional stability, and chemical resistance in the material. In Fig. 4(c), the FTIR spectra of cotton waste, MCC, and CMCC are highly similar, with absorption bands at 3 342 cm^{-1} (O—H stretching), 2 905 cm^{-1} (C—H stretching), 1 313 cm^{-1} (C—H bending), 1 025 cm^{-1} (C—O—C stretching), and 897 cm^{-1} (β-glycosidic linkage vibration). The absorption band at 1 631 cm^{-1} is assigned to the O—H bending vibration of adsorbed water, which is a common feature due to the strong hydrophilicity of the abundant hydroxyl groups on the cellulose chains. The characteristic β-glycosidic linkage of cellulose I at 897 cm^{-1} shows no significant change across all samples, indicating that the alkali treatment and acid hydrolysis effectively removed non-cellulosic impurities and amorphous regions without altering or damaging the fundamental cellulose molecular skeleton. Figure 4(d) reveals that MCC begins to degrade at 203 ℃, with a maximum decomposition temperature of 377 ℃. The thermal degradation from onset to maximum decomposition involves dehydration, decarboxylation, depolymerization, and glucosyl unit cleavage, ultimately forming carbonized residues. Compared with cotton waste, MCC exhibits a lower thermal decomposition temperature, which is mainly because sulfuric acid hydrolysis cleaved the long cellulose chains, significantly reducing the degree of polymerization. Additionally, trace sulfate groups ($—OSO_3H$) introduced on the surface during the acid treatment acted as catalysts, further accelerating the thermal degradation at lower temperatures.

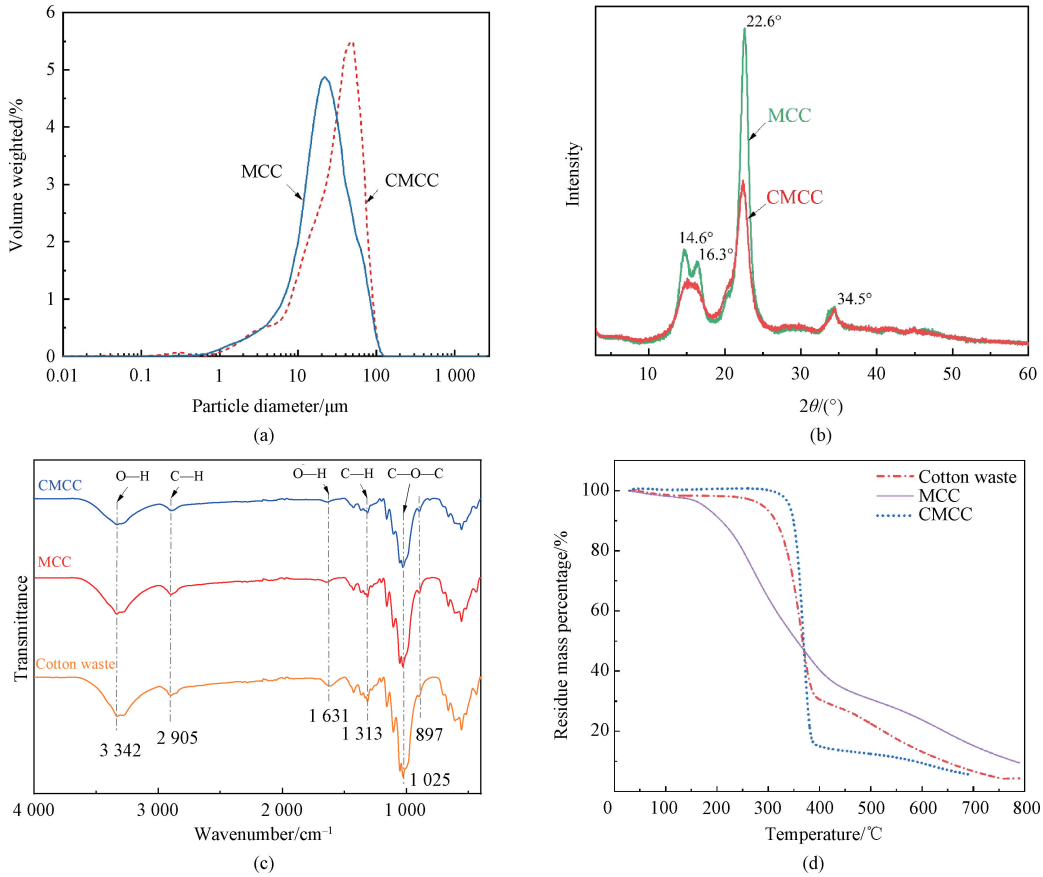


Fig. 4 Physicochemical characterization results of samples: (a) particle size distributions of MCC and CMCC; (b) XRD patterns of MCC and CMCC; (c) FTIR spectra of cotton waste, MCC, and CMCC; (d) TG curves of cotton waste, MCC, and CMCC

2.2 Tensile properties of composites

Figure 5 presents a comparison of the tensile properties of jute/glass fiber-reinforced epoxy composites before and after MCC addition. After incorporating 4% MCC, the tensile properties of the non-hybrid composites (8G and 4J) are comparable to or slightly lower than those without MCC. In contrast, the hybrid composites (2G1J2G1J and 2G2J2G) exhibit comparable or slightly higher tensile properties relative to their non-MCC counterparts. This is related to the modification mechanism of MCC and the interfacial characteristics of the different fibers.

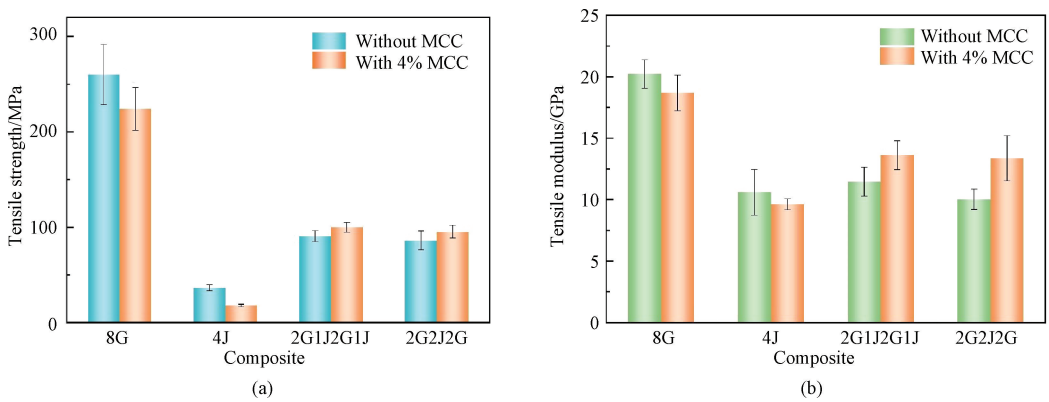


Fig. 5 Tensile properties of composites: (a) tensile strength; (b) tensile modulus

For the 8G and 4J composites, due to the single reinforcement structure, some MCC particles agglomerate on the fiber surface, and this negative effect outweighs the interaction between the hydroxyl groups of MCC and those of the fibers. The agglomerated MCC acts as stress concentration points, resulting in reduced tensile strength and modulus.

For the hybrid composites, 2G1J2G1J and 2G2J2G,

MCC is well dispersed within the hybrid system, increasing the contact area between the fabric and the epoxy resin. Moreover, the abundant hydroxyl groups on MCC can form hydrogen bonds with those on the jute and glass fibers. These synergistic effects enhance the interfacial adhesion between the two dissimilar fibers and the epoxy resin. Consequently, stress transfer across the interface is facilitated, leading to improved mechanical properties.

In addition, regardless of the presence of MCC, the 8G composite exhibits the highest tensile strength and tensile modulus, with maximum values of 254.94 MPa and 20.21 GPa, respectively, owing to the inherent high strength and modulus of glass fibers. Meanwhile, compared with the 4J composite, the tensile strengths of the hybrid composites are improved, demonstrating that the introduction of glass fibers is a key factor in enhancing the tensile properties of the material.

Figure 6 shows the microscopic images of the tensile fracture morphologies of the composites with different stacking sequences before and after MCC addition. As marked by the red circles in Fig. 6(a), without MCC, 2G1J2G1J exhibits obvious interfacial delamination and irregular fibers at the tensile fracture surface; 2G2J2G shows even more pronounced delamination, occurring not only between glass fibers but also between glass fiber fabric and jute fabric, with a distinct fracture surface. As circled in Fig. 6(b), after adding 4% MCC, 2G1J2G1J presents a flat tensile fracture surface with some interphase cracks but no significant delamination; meanwhile, no delamination is observed between glass fiber fabric and jute fabric in 2G2J2G, indicating good interfacial bonding.

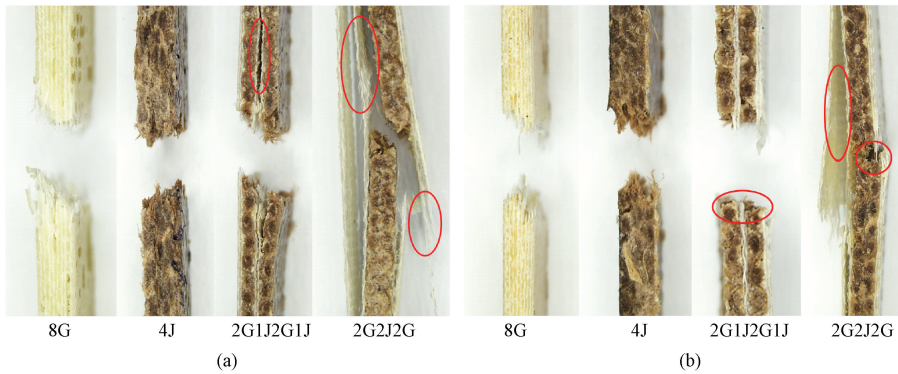


Fig. 6 Microscopic photograph of composites' microstructure after tensile failure: (a) without MCC; (b) with 4% MCC

2.3 Bending properties of composites

Figure 7 presents a comparison of the bending strength and modulus of jute/glass fiber-reinforced epoxy composites before and after MCC addition. After adding 4% MCC, except for a decrease in the bending strength of 4J, the bending strengths of the other three composites and the bending moduli of all four composites exhibit comparable or improved levels. The opposite tensile/bending responses of 8G composites to MCC arise from distinct stress transfer modes. MCC suppresses interfacial cracking under bending loading via hydrogen bonding, enhancing strength and modulus. Under tensile loading, particle-induced stress concentration and micro-voids dominate, reducing tensile performance despite improved interfacial adhesion. Notably, both hybrid composites (2G1J2G1J and 2G2J2G) exhibit significantly enhanced bending strengths and moduli after MCC addition. This improvement is attributed to the abundant hydroxyl groups of MCC, which form hydrogen bonds or physical crosslinks with the hydroxyl groups of the fibers and the epoxy resin, leading to tighter interfacial bonding and thus improved bending properties.

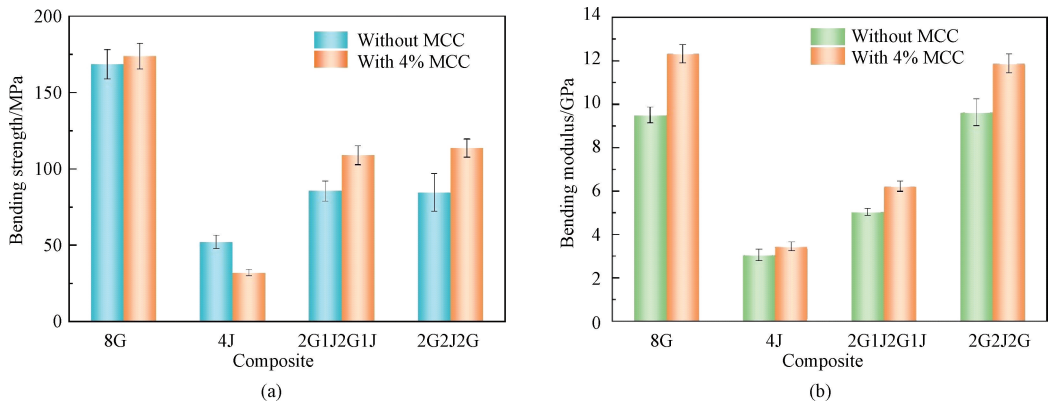


Fig. 7 Bending properties of composites: (a) bending strength; (b) bending modulus

The bending properties of 2G1J2G1J and 2G2J2G fall within the range spanned by 8G and 4J. 2G2J2G shows a higher bending modulus than 2G1J2G1J. After MCC addition, the bending strength and modulus of 2G2J2G reached 113.66 MPa and 11.87 GPa, respectively, which were 34.19% and 23.26% higher than those of the non-MCC composites. This difference was mainly attributed to the effects of fabric stacking sequence and structural symmetry.

2.4 Fracture morphology analysis

Figure 8 shows SEM images of the bending fracture cross-sections of the composites before and after MCC addition. As shown in Figs. 8(a) and 8(b), 8G without MCC exhibits obvious interfacial delamination at the bending fracture, whereas after adding 4% MCC, no delamination is observed and fewer fibers are pulled out, which is closely related to the improved interfacial properties due to MCC. From Figs. 8(c) and 8(d), 4J without MCC shows good wetting between fiber bundles and resin at the bending fracture. However, after adding 4% MCC, a large number of pulled-out fibers appear on the fracture surface, indicating that MCC does not provide significant interfacial reinforcement but rather hinders resin wetting, thereby reducing the bending strength of 4J. The opposite effects of MCC on the flexural fracture behaviors of 8G and 4J composites arise from the fundamental differences in surface chemistry and morphology between glass and jute fibers. MCC improves 8G by hydrogen-bonding at the smooth glass interface, but weakens 4J by physically blocking the porous jute surface and hindering resin penetration, which turns mechanical interlocking into weak particle-bridging.

For the two hybrid fiber-reinforced composites, without MCC (Figs. 8(e) and 8(g)), many pulled-out jute and glass fibers are observed at the bending fracture, along with obvious interfacial delamination. After adding 4% MCC (Figs. 8(f) and 8(h)), resin wetting on the fracture surface is enhanced. Neither 2G1J2G1J nor 2G2J2G exhibits interfacial delamination, and the layers of 2G2J2G were more tightly bonded, indicating good interfacial adhesion between the fibers and the epoxy resin. The SEM observations were in good agreement with the bending properties.

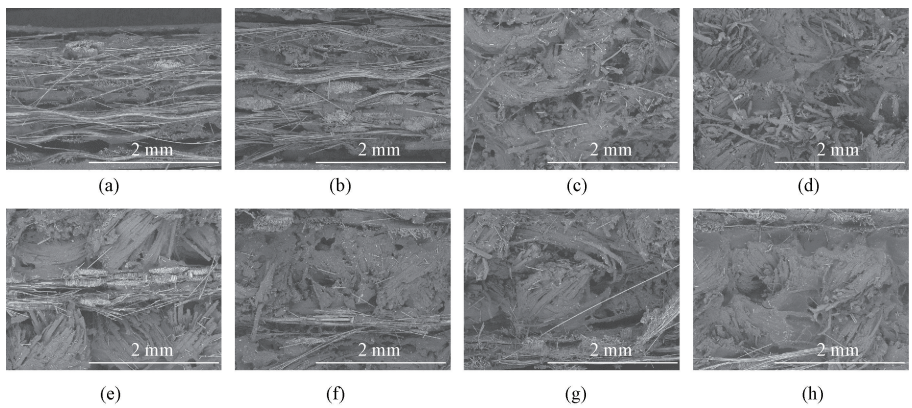


Fig. 8 SEM images of bending fracture cross-sections of composites before and after MCC addition: (a) 8G without MCC; (b) 8G with 4% MCC; (c) 4J without MCC; (d) 4J with 4% MCC; (e) 2G1J2G1J without MCC; (f) 2G1J2G1J with 4% MCC; (g) 2G2J2G without MCC; (h) 2G2J2G with 4% MCC

Figure 9 shows SEM images of the bending fracture cross-section of 2G2J2G with 4% MCC at magnifications of 100× and 200×. As seen in Fig. 9(a), after adding 4% MCC, the interfaces between the glass fibers, jute fibers, and epoxy resin are tightly bonded; the fibers are well wetted by the resin, and only a few glass fibers are pulled out. In Fig. 9(b), MCC particles wrapped by epoxy resin are observed on the surface of the 2G2J2G (marked by yellow circles), indicating that an appropriate amount of MCC can be well dispersed in the epoxy resin. Unlike in the jute-only system (4J), where MCC particles physically block the porous jute surface and hinder resin penetration, in the hybrid system, MCC adheres to both jute and glass fiber fabrics via hydrogen bonding. The glass fibers, with their smooth inorganic surface, provide favorable sites for MCC anchoring, thereby mitigating the pore-blocking effect on jute. Moreover, the large specific surface area of MCC increases the fiber-resin contact area. Consequently, MCC synergistically enhances the interfacial interaction between the fibers and the epoxy resin, reduces stress concentration, and promotes load transfer. This synergistic effect is particularly pronounced in the structurally symmetric 2G2J2G hybrid layup system.

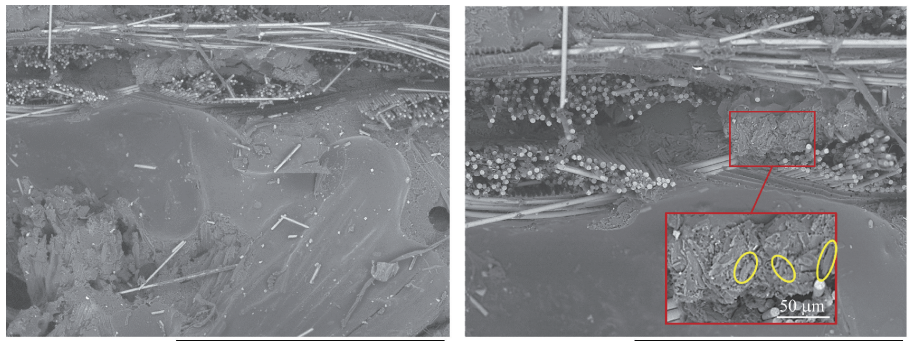


Fig. 9 SEM images of 2G2J2G with 4% MCC at different magnifications: (a) 100×; (b) 200×

3 Conclusions

In this study, four types of jute/glass fiber-reinforced epoxy composites with different stacking sequences were designed. MCC was interlayered to improve the composite interface, and the composites with and without MCC treatment were fabricated. The prepared MCC exhibits a ribbon-shaped or rod-shaped morphology at the micrometer scale, with an average particle size of 26.53 μm, a crystallinity of 89.53%, and an initial decomposition temperature of 203 ℃, surpassing the corresponding properties of CMCC.

After adding MCC, the mechanical properties of the hybrid composites improved. Compared with the unmodified composite, the bending strength and modulus of 2G2J2G increased by 34.19% and 23.26%, respectively. This is attributed to the formation of hydrogen bonds and mechanical interlocking between the MCC, jute fibers, and glass fibers. Additionally, the large specific surface area of MCC provides a larger effective contact area between the fibers and the epoxy resin matrix, thereby enhancing interfacial bonding strength, facilitating efficient stress transfer, and suppressing delamination. In this study, cotton waste was effectively upcycled into MCC, which enhanced the interfacial properties of the hybrid composites. Benefiting from this improvement, the developed hybrid composites show great promise for infrastructure applications, such as door and window frames, as well as automotive components, including door panels and dashboards. These results demonstrate that the hybridization of glass and jute fibers, together with the appropriate amount of MCC, offers a cost-effective and sustainable approach to producing high-performance composites for lightweight structural applications.

References

[1] Dinkar V C, Kumar V. A review study on the mechanical behaviour of natural fibre-reinforced epoxy composite [J]. *Polymer Bulletin*, 2025, 82(15): 9647-9682.

[2] Arumugam S, Kandasamy J, Venkatesan S, et al. A review on the effect of fabric reinforcement on strength enhancement of natural fiber composites [J]. *Materials*, 2022, 15(9): 3025.

[3] Wang Y N, Sultana J, Rahman M M, et al. A sustainable and biodegradable building block: review on mechanical properties of bamboo fibre reinforced PLA polymer composites and their emerging applications [J]. *Fibers and Polymers*, 2022, 23(12): 3317-3342.

[4] Balaji D, Arulmurugan B, Bhuvaneswari V. An overview of the additive manufacturing of bast fiber-reinforced composites and envisaging advancements using the patent landscape [J]. *Polymers*, 2023, 15(22): 4435.

[5] Nautiyal S, Dimri S, Riyal I, et al. Natural fibres and their composites: a review of chemical composition, properties, retting methods, and industrial applications [J]. *Cellulose*, 2025, 32(6): 3497-3527.

[6] Dönitz A, Köllner A, Richter T, et al. Additive manufacturing of biodegradable hemp-reinforced polybutylene succinate (PBS) and its mechanical characterization [J]. *Polymers*, 2023, 15(10): 2271.

[7] Sudha, G S, Aswathy N R, Biswal M C, et al. Investigating the reinforcing effect of jute fiber in a PLA & PBAT biopolymer blend matrix for advanced engineering applications: enhancing sustainability with bioresources [J]. *Materials Today Communications*, 2024, 40: 109960.

[8] Mahaninia M H, Yan N. Chitosan-based partial vitrimer for making eco-friendly multifunctional ramie fabric reinforced composite [J]. *International Journal of Biological Macromolecules*, 2025, 309: 142979.

[9] Tahir D, Fatima N, Rehan M, et al. Sustainable jute fiber-reinforced auxetic composites with both in-plane and out-of-plane auxetic behaviors [J]. *Polymer Composites*, 2025, 46(S1): S922-

S939.
[10] Suriani M J, Ilyas R A, Zuhri M Y M, et al. Critical review of natural fiber reinforced hybrid composites: processing, properties, applications and cost [J]. *Polymers*, 2021, 13(20): 3514.
[11] Saha S, Das S, Rahman M Z. Hybridization in natural fiber composites: enhanced performance and sustainability [J]. *Composites Part B: Engineering*, 2026, 308: 112986.
[12] Karademir C, Tanarslan H M, Yalçınkaya Ç, et al. Development of sustainable polymer composites containing waste glass and natural fibers for strengthening purposes [J]. *Polymers*, 2025, 17(8): 1116.
[13] Yang L J, Wang H G, Wu H, et al. Research progress on high performance of natural fiber reinforced plastic based on fiber modification method [J]. *New Chemical Materials*, 2021, 49(12): 67-72. (in Chinese)
[14] Kumar S, Prasad L, Patel V K, et al. Physical and mechanical properties of natural leaf fiber-reinforced epoxy polyester composites [J]. *Polymers*, 2021, 13(9): 1369.
[15] Dilfi K F A, Balan A, Bin H, et al. Effect of surface modification of jute fiber on the mechanical properties and durability of jute fiber-reinforced epoxy composites [J]. *Polymer Composites*, 2018, 39(S4): E2519-E2528.
[16] Shadhin M, Tisha N J, Dulal M, et al. Adhesion chemistry of plant-based cellulosic fibers and polymeric matrices in composites: a review [J]. *RSC Advances*, 2026, 16(7): 6132-6163.
[17] Lal S S, Kannan S. Influence of microcrystalline cellulose on curing kinetics, mechanical and thermo-mechanical properties of epoxy methyl ricinoleate toughened epoxy copolymer [J]. *Journal of Polymers and the Environment*, 2024, 32(2): 913-934.
[18] Rehman M M, Zeeshan M, Shaker K, et al. Effect of micro-crystalline cellulose particles on mechanical properties of alkaline treated jute fabric reinforced green epoxy composite [J]. *Cellulose*, 2019, 26(17): 9057-9069.
[19] Jabbar A, Militký J, Wiener J, et al. Nanocellulose coated woven jute/green epoxy composites: characterization of mechanical and dynamic mechanical behavior [J]. *Composite Structures*, 2017, 161: 340-349.
[20] Asadi A, Miller M, Moon R J, et al. Improving the interfacial and mechanical properties of short glass fiber/epoxy composites by coating the glass fibers with cellulose nanocrystals [J]. *Express Polymer Letters*, 2016, 10(7): 587-597.
[21] Bandaru A K, Pichandi S, Ma H, et al. Effect of microcrystalline cellulose on the mechanical properties of flax reinforced methylmethacrylate and urethane acrylate composites [J]. *Journal of Materials Science*, 2024, 59(7): 2872-2892.

落棉 MCC 对黄麻/玻纤增强环氧复合材料界面及力学性能的影响

李宏扬，杨家骅，王泽川，姚　澜，王　妮*
东华大学 纺织学院，上海 201620

摘　要：由于能源短缺和环境污染问题日益突出，开发可用于基础设施和汽车等领域的天然纤维增强复合材料已势在必行。本研究采用低成本的天然黄麻纤维作为复合材料增强体，为进一步提升整体力学性能，引入少量玻璃纤维，制备了混杂复合材料。为改善纤维与环氧树脂之间的界面性能，采用由落棉制备的微晶纤维素(microcrystalline cellulose，MCC)对复合材料进行改性处理。引入 MCC 改变了所设计的 4 种黄麻/玻璃纤维增强环氧复合材料力学性能。特别是上下表层各为 2 层玻璃纤维织物、中间为 2 层黄麻织物的复合材料(命名为 2G2J2G)，引入 MCC 后，其弯曲强度与弯曲模量分别达到 113.66 MPa 和 11.87 GPa，较未添加 MCC 的复合材料分别提升了 34.19% 和 23.26%。扫描电子显微镜观察表明，MCC 在树脂基体中分散均匀，这对复合材料界面性能的增强产生了积极作用。

关键词：天然纤维增强复合材料；微晶纤维素；黄麻；玻璃纤维；界面性能